Advance Research in Textile Engineering

Open Access

Austin Publishing Group

Research Article

Contributions of Surround Conditions on Color Appearance of Peridot Based on CAM16 Prediction

Liu K[1], Tang J[1]*, Guo Y[1], Shang Y[1] and Bi J[2]
[1]School of Gemmology, China University of Geosciences (Beijing), China
[2]Qingdao Congyuan Culture Co., Ltd, China

***Corresponding author:** Jun Tang, School of Gemmology, China University of Geosciences (Beijing), No. 23 Xueyuan Road, Haidian District, Beijing, China

Received: April 25, 2022; **Accepted:** May 12, 2022; **Published:** May 19, 2022

Abstract

Peridot is the most abundant mineral on the earth and is widely used as gemstone in the world. In this paper, EMP analysis, UV-vis spectroscopy, and X-Rite SP62 spectrophotometer were used to study the chemical composition and color of the peridot. The CAM16 model was applied to predict the color appearance of peridot in different surrounding conditions. The chemical analysis and UV-vis spectra analysis showed there are seven narrow absorption bands at 414nm, 443nm, 481nm, 512nm, 557nm, 664nm and 684nm in peridot that should be assigned to the Fe chromophore. The color predictions indicated that the peridot will be brighter and more vivid when the luminance increases, which corresponds to Hunt Effect and Stevens Effect. Viewing surroundings have a great influence on the lightness and brightness in color appearance of peridot. CAM16 color appearance model is not suitable to predict the contributions of the light source on the color appearance of peridot due to the metameric effect. The windowing issue and the facets in peridot should be taken into consideration during the prediction calculation.

Keywords: Peridot; Color vision; CAM16

Introduction

Peridot is the most abundant mineral [1] on the earth and is usually used as a gemstone for decoration. Commercially important sources such as United States [1]; China [2,3]; Pakistan [4-7]; Myanmar [8-10]; Vietnam [11,12]; Tanzania [13,14]; Egypt [9,15]; Italy [16], and Sri Lanka [17]. Peridot was famous for its beautiful yellowish-green color, and it has been used for about 3,000 years, but there are quite a few researches available on the color of this ancient gemstone.

Peridot color is easily influenced by environmental conditions. In our previous research, we studied the objective color effect of luminance [18], light source [19], and background [20] on the color appearance of peridot. However, these basic colorimetry researches only provide the fundamental color measurement results. While color appearance phenomenon appears when we observe an object in a specific environment. Color research of peridot will be more applicable when color psychology is taken into consideration.

To study the subjective color effect of the human eye, great effort has been made by many scientists. A color appearance model, CIECAM97s, was recommended by CIE (Commission Internationale de L'Eclairage) in 1997 [21]. Soon the CIE recommended a new model named CIECAM02 in 2004 [22,23]. It removed many shortcomings from CIECAM97s and improved the predictions of the color appearance datasets. CIECAM02 color appearance model was widely used around the world for over ten years. Until 2017, a newly derived color appearance model, named CAM16, was recommended by Li et al. [24]. It was not only overcoming the previous problems but also does well in predicting the results from visual experiments. CAM16 is considered the most precise color appearance model so far [25,26].

This paper presents the predicted color appearance of peridot by applying the forward CAM16 model, compared to the color data in the previous research.

Materials and Methods

Materials

The 95 pieces of faceted peridot from China, Pakistan, and Myanmar, ranging from 1.02 to 13.65 ct with high purity, display an even color of yellowish-green with continuous changes of color appearance and depth.

Colorimetric analysis

X-Rite SP62 spectrophotometer was used to collect reflective signals from the peridot surface via the integrating sphere. Test conditions were described as follows: reflection, not including the specular reflection, the observer view of 2°, measuring range from 400nm to 700nm, measuring time: less than 2.5 sec, wavelength interval:10nm; voltage: 220V; frequency:50-60 Hz.

Electron Microprobe (EMP) analysis

Major element compositions of peridots were analyzed using a JXA-8230 electron microprobe at the Beijing ZKKY GeoAnalysis Laboratory Co., Ltd. The operating conditions were accelerating voltage of 15kV for silicate and oxide, and 20kV for sulfide, beam current of 20nA, and beam size of 5μm. Natural minerals and synthetic oxides were used as standards. Matrix corrections were carried out using the ZAF correction program supplied by the manufacturer.

UV-vis absorption spectroscopy

Ultraviolet-visible spectrums were measured in the 300 to 800 nm range using a UV-3600 UV-vis spectrophotometer and a 0.5nm spectral resolution at a scan speed of 400nm/min. The detector conversion wavelength is 850nm and the grating conversion wavelength is 900nm with S/R shift.

Citation: Liu K, Tang J, Guo Y, Shang Y and Bi J. Contributions of Surround Conditions on Color Appearance of Peridot Based on CAM16 Prediction. Adv Res Text Eng. 2022; 7(1): 1071.

Forward CAM16 Color Appearance Model

Color appearance parameters of peridot were calculated by the forward CAM16 color appearance model, which was established by Li et al., [24]. Detailed algorithm sees in the supplemental document 1. In this model, four groups of parameters, including luminance, light source, background, and viewing surroundings, were considered as test parameters.

Results and Discussions

Chemical analysis

The chemical compositions of the studied peridots were measured using EMP. The results are shown in Table 1, confirming the gem-quality peridot belongs to the forsterite series. The results show that Fe is the most important chromophore in peridot, more evidences will be presented in the following analysis.

UV-vis spectra

The recorded UV-vis absorption spectra (Figure 1) of the peridots are in agreement with previously published data [27], showing seven narrow absorption bands at 414nm, 443nm, 481nm, 512nm, 557nm, 664nm, and 684nm. These absorptions bands are assigned to the Fe chromophore. The spectra show the peridot mainly reflects green and yellow light, which corresponds to the yellowish-green color of the peridot in daylight.

Color contributions of surrounding conditions

Color tristimulus values of peridot were tested by spectrophotometer and used for calculation. Based on the CAM16 color appearance model, we calculated the color appearance data of peridot by changing a single variate of surround parameters.

Luminance: In our previous research, we designed an experiment (Figure 2A) to study the objective color effect of illuminance on the color of peridot. We set up six levels of illuminance including 500lx, 1000lx, 1500lx, 2000lx, 2500lx and 3000lx. In this paper, the illuminance data (lx) should be converted into luminance data (cd/m^2). According to the Grey World Hypothesis [28]:

$$L_A = E/5\pi \quad (1)$$

In the formula, L_A represents luminance, and E represents

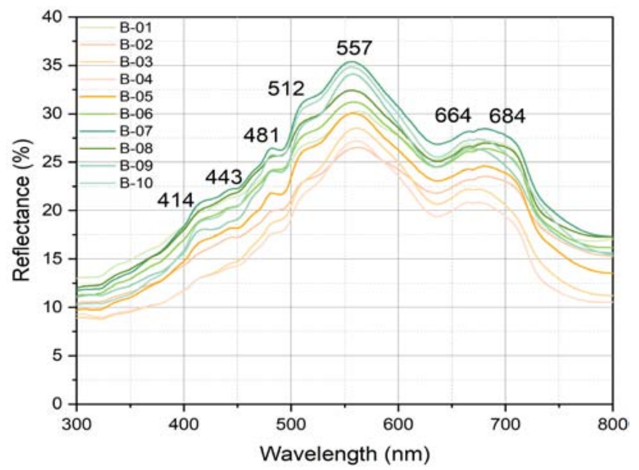

Figure 1: UV-vis spectra of the studied peridot samples.

Table 1: EMP analysis data of the studied peridot samples.

Sample	B-01	B-02	B-03	B-04	B-05	B-06	B-07	B-08	B-09	B-10
wt% Oxides										
SiO_2	41.778	41.937	41.004	41.674	41.691	41.592	42.032	40.728	41.723	41.433
TiO_2	0.013	0.015	0.000	0.000	0.027	0.024	0.034	0.000	0.000	0.029
Al_2O_3	0.040	0.022	0.068	0.038	0.104	0.021	0.039	0.022	0.031	0.040
Cr_2O_3	0.036	0.006	0.036	0.029	0.038	0.066	0.024	0.012	0.000	0.000
$FeO_{(total)}$	9.695	9.083	8.856	9.441	9.575	10.037	9.579	8.714	9.279	10.009
MnO	0.133	0.136	0.173	0.151	0.103	0.132	0.113	0.128	0.127	0.147
MgO	47.825	48.408	49.443	48.302	48.088	47.731	47.858	49.983	48.548	48.040
NiO	0.408	0.331	0.342	0.314	0.321	0.282	0.264	0.320	0.236	0.251
CaO	0.071	0.061	0.078	0.050	0.052	0.114	0.057	0.093	0.055	0.051
Cations on the basis of 4 O atoms per formula unit										
Si	1.021	1.022	1.001	1.018	1.018	1.019	1.026	0.995	1.018	1.015
Ti	0.000	0.000	0.000	0.000	0.001	0.000	0.001	0.000	0.000	0.001
Al	0.001	0.001	0.002	0.001	0.003	0.001	0.001	0.001	0.001	0.001
Cr	0.001	0.000	0.001	0.001	0.001	0.001	0.001	0.000	0.000	0.000
Fe	0.198	0.185	0.181	0.193	0.196	0.206	0.196	0.178	0.189	0.205
Mn	0.003	0.003	0.004	0.003	0.002	0.003	0.002	0.003	0.003	0.003
Mg	1.743	1.759	1.800	1.759	1.751	1.742	1.741	1.820	1.765	1.754
Ni	0.008	0.007	0.007	0.006	0.006	0.006	0.005	0.006	0.005	0.005
Ca	0.002	0.002	0.002	0.001	0.001	0.003	0.002	0.002	0.001	0.001
Total	2.977	2.977	2.997	2.981	2.979	2.980	2.973	3.005	2.982	2.984

illuminance. Corresponding to the six levels of illuminance, the luminance data should be 31.8310cd/m^2, 63.6620cd/m^2, 95.4930cd/m^2, 127.3240cd/m^2, 15 9.1549cd/m^2 and 190.9859cd/m^2, respectively (Figure 2B). Except for luminance, we chose a D65 light source, Munsell N7 background (neutral gray, Y_b=43.06), and "Average" viewing surrounds to calculate the color appearance of the peridot.

The prediction results indicate that brightness Q rises with luminance and lightness J is used as a constant (Figure 2C), which corresponds to the Stevens Effect that relative brightness rises with relative luminance. Actual measurement to lightness L^* also shows an uptrend. It is the same as what we observe using our naked eyes. As for hue h and hue angle h°, they are closed to each other and show a slight downtrend when the luminance rises (Figure 2D), which corresponds to the Bezold-Brücke Hue Shift phenomenon that is a perceptual change in hue when the intensity of a stimulus is increased or decreased. Chroma C remains constant, while chroma C^* rises when luminance increases from 31.8310cd/m^2 to 159.1549 cd/m^2 and then goes down (Figure 2E). We believe that the chroma C^* goes down because too much white light reflects from the facets of the peridot due to the cut quality. Besides, the value of colorfulness M goes up with luminance, which corresponds to Hunt Effect which is a perceptual change in chromaticity. While saturation s decreases with luminance, which is believed to be due to the reduction of brightness (Figure 2F).

The color appearance data of peridot predicted by the CAM16 color appearance model is closed to that we had a test in our previous research. It is found that the color appearance of peridot will be

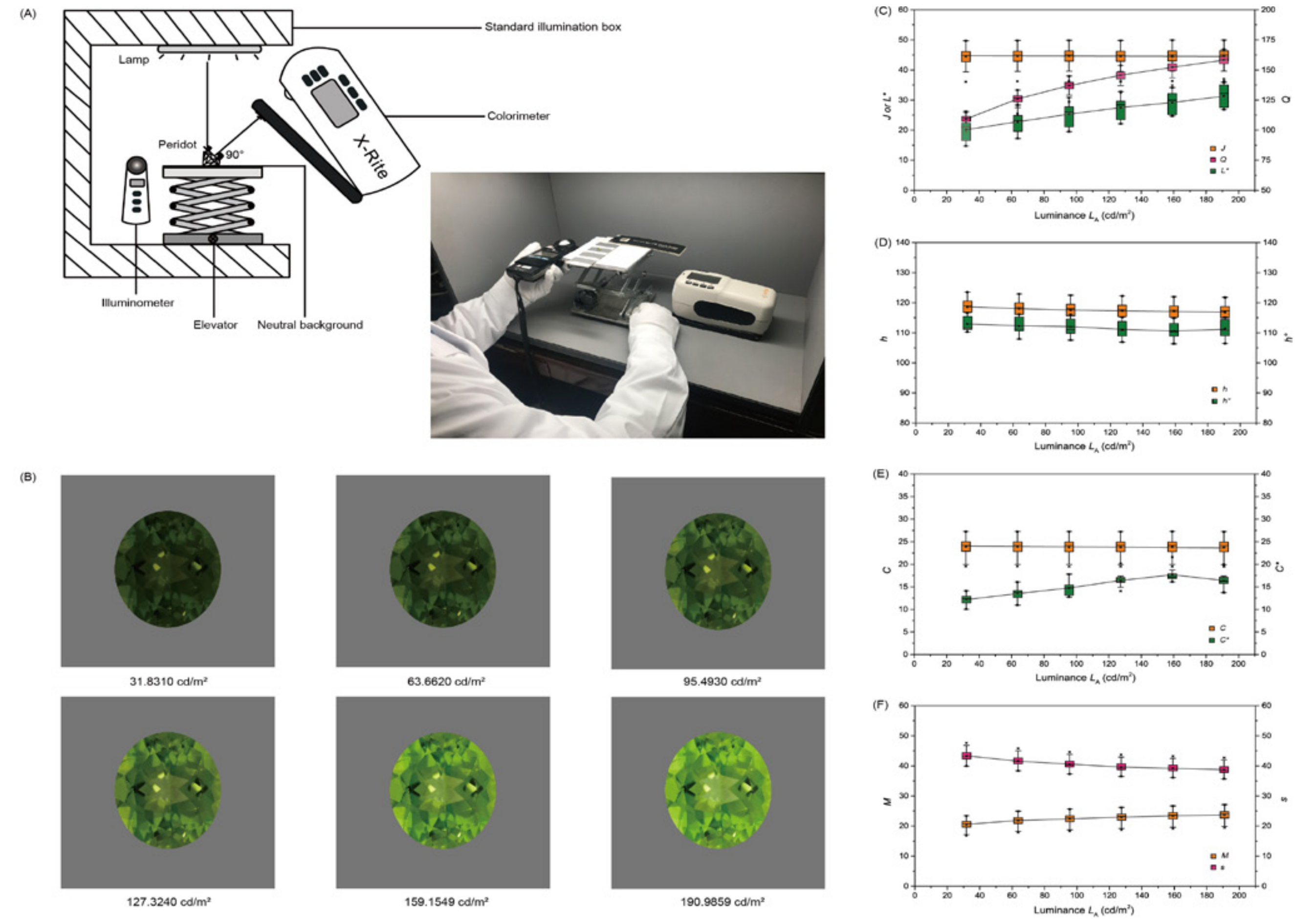

Figure 2: Effect of luminance on the color appearance of peridot. We designed an experiment in our previous research (Tang, Guo & Xu, 2018) to test the color data of peridot in different luminance; (A) Pictures of peridot in different luminance are shown in figure; (B) Relationship between luminance and lightness *J*, L^*, brightness *Q*; (C); hue *h*, hue angle *h*°; (D) Chroma *C*, C^*; (E) colorfulness *M* and saturations; (F) are given.

brighter and more vivid when the luminance is increased. However, the particularity of gemstones such as facets should be taken into consideration when we evaluate their color appearance.

Light Source: Six kinds of standard light sources including A (2856K, PHILIPS HALOGENA 60W/230V, France), F12(3000K, PHILIPS F20T12/30U 20W, USA), F11(4000K, PHILIPS MASTER TL-D 18W/840, Holland), F2(4230K, PHILIPS TL-D 18W/33, Holland), D50(5003K, PHILIPS TL-D 90 De Luxe Pro 18W/950, Holland), and D65(6504K, PHILIPS MASTER TL-D 90 De Luxe 18W/965, Holland) were used to study the effect of the light source on the color appearance of peridot (Figure 3K).

The results show that there has no significant difference in lightness *J* (Figure 3A), brightness *Q* (Figure 3B), and lightness L^* (Figure 3C) under six kinds of the standard light source, which indicates that the light source has no great effect on the color appearance of peridot. Prediction results of chroma *C* (Figure 3D), colorfulness *M* (Figure 3E) and saturation s (Figure 3F) show the same trend from high to low: A, F12, D65, F11, F2, and D50 respectively. On the contrary, the actual measurement of chroma C^* shows a different result (Figure 3G). This conformity phenomenon is believed to be caused by the metameric effect that a color-change effect due to the Spectral Power Distribution (SPD) of the light source (Figure 3J) and the selective absorption of visible light in peridot. Similarly, the difference between hue *h* (Figure 3H) and hue angle *h*° (Figure 3I) of peridot is also caused by the metameric effect.

There has a difference between results predicted by the CAM16 color appearance model and actual measurement results when we study the effect of the light source on the color appearance of peridot, the reason which is due to the metameric effect. Therefore, the CAM16 color appearance model maybe not apply to the study of the effect of the light source on the color appearance of peridot, even gemstones.

Background: The color appearance model can only predict the color appearance of an object on the different grayscale background colors. In previous research, we used Munsell neutral color chips to study the objective effect of background on the color appearance of peridot. Munsell neutral color chips are composed of 37 neutral gray colors with different lightness from N0.5 to N9.5. N1, N2, N3, N4, N5, N6, N7, N8, and N9 color chips are used as background (Figure 4B) whose lightness and luminance factors are shown in Table 1. The lightness of Munsell neutral background has a power relationship with its luminance factor (Figure 4A):

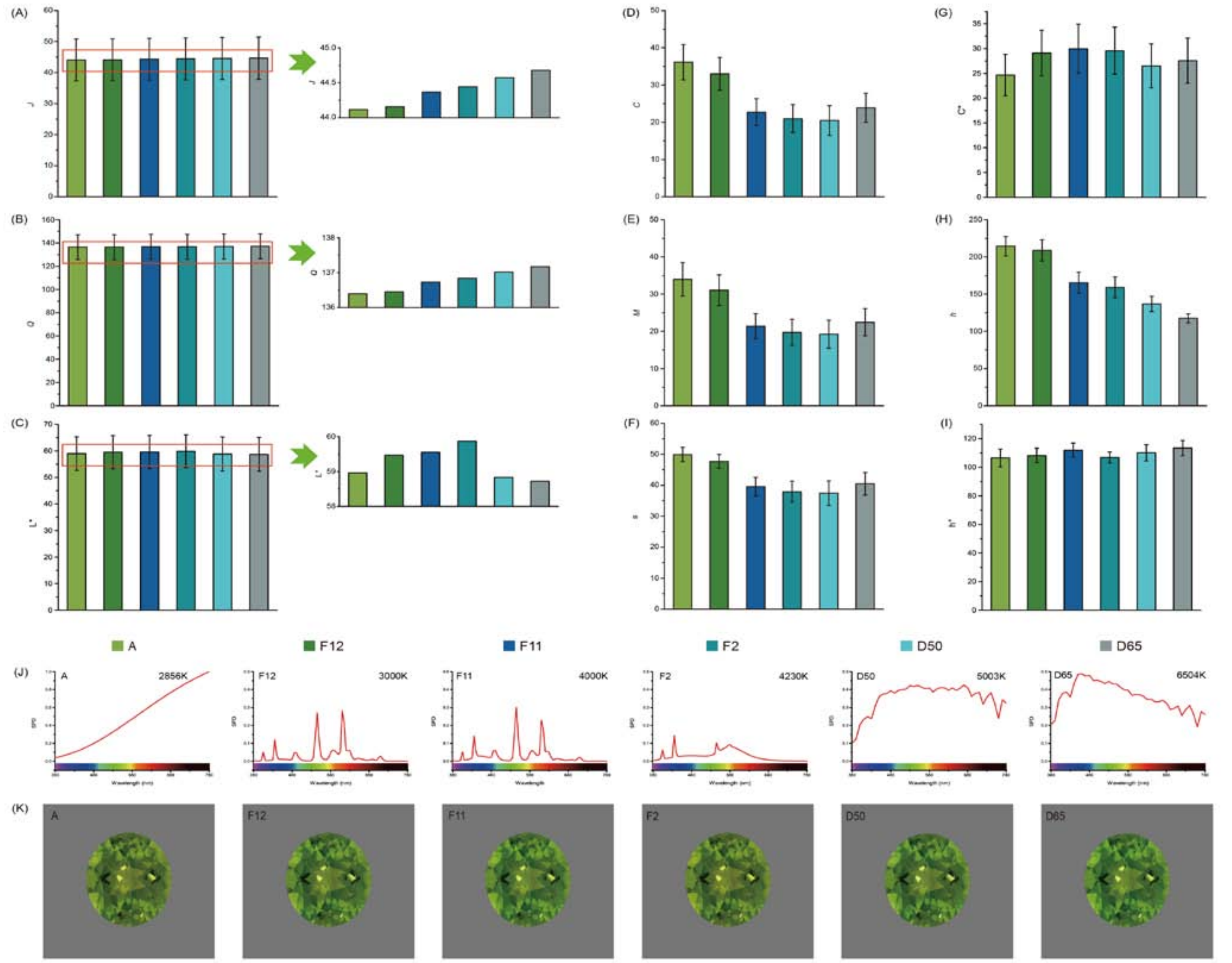

Figure 3: Effect of the light source on the color appearance of peridot. Lightness *J;* (A) brightness *Q;* (B) lightness L^*; (C) chroma *C;* (D) colorfulness *M*; (E) saturation *s*; (F) Chroma C^*; (G) hue *h* ;(H) and hue angle *h°*; (I) of peridot in different light sources are given; (J) The spectral power distribution of six standard light sources; (K) Pictures of peridot in different light sources.

$$L^*_b=116Y_b^{1/3}-16 \qquad (2)$$

L_b^* represents the lightness of the background, and Y_b represents the luminance factor of the background.

The results indicate that lightness *J* and brightness *Q* fall with the increase of the luminance factor of the background. However, it's quite different from the value of actual measurement to lightness L^* of peridot in the different neutral backgrounds rises with luminance factor of background, which is believed to be due to the transparency and cut quality of peridot (Figure 4C). Most of the gemstones will be cut into faceted stones for maximizing their beauty. But not all of them will be cut into perfect proportion for reducing weight loss, which makes gemstones show windowing. The color of gemstones will not be influenced by background color when the gemstones are well-cut. We believed that these results were most likely due to the windowing issue of peridot. The chroma *C* (Figure 4D) and colorfulness *M* (Figure 4E) fall with the increase in the luminance factor of the background. But actual measurement of chroma C^* (Figure 4D) rises with the luminance factor of the background. Similarly, this phenomenon should be explained by the windowing issue in peridot. More light will be reflected into the peridot when the luminance factor increases so which improves the luminance of the peridot and then enhances the chroma due to Hunt Effect. The increase in saturation s should be explained by the decrease in brightness. There has no significant effect on the hue of the color of peridot by the lightness of the background color.

CAM16 color appearance model is probably not suitable to predict the color appearance of peridot, the windowing issue in peridot should be taken into consideration during prediction calculation.

Viewing Surrounds: CAM16 color appearance model defines three viewing surrounds: Dark, Dim, and Average. These three surrounding conditions are linear correlated and quantified by three surrounding parameters: *F*, *c*, and N_c (Figure 5A). *F* is the maximum degree of adaptation, *c* is an exponential nonlinearity, and N_c is the chromatic induction factor. The viewing surroundings are used to

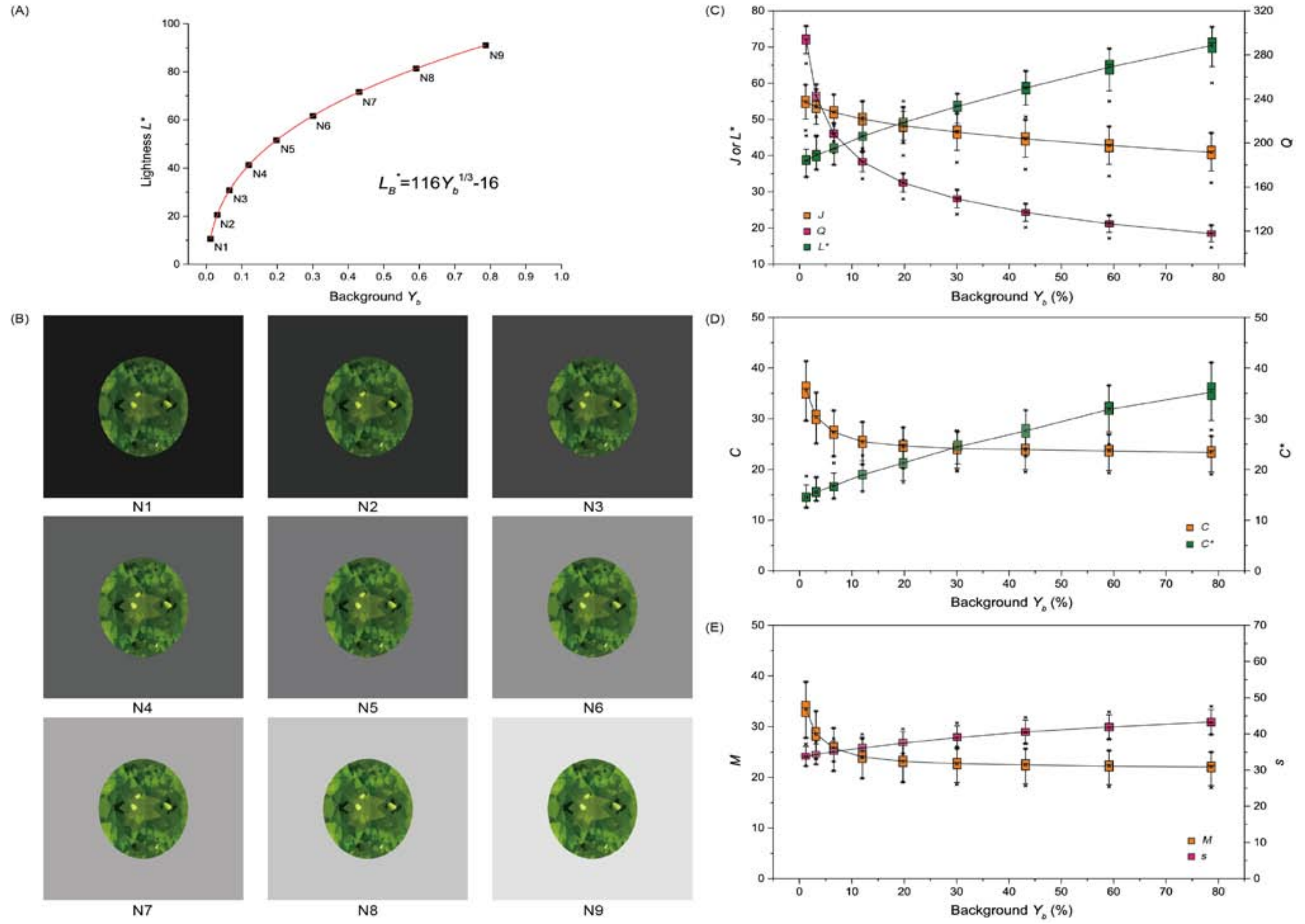

Figure 4: Effect of background on the color appearance of peridot. (A) A power function relation exists between the background brightness factor and lightness; (B) Pictures of peridot on different grayscale backgrounds. Relationship of background brightness factor between lightness *J*, L^*, brightness *Q*; (C) chroma *C*, C^*; (D) colorfulness *M*, and saturation *s* (E) of peridot.

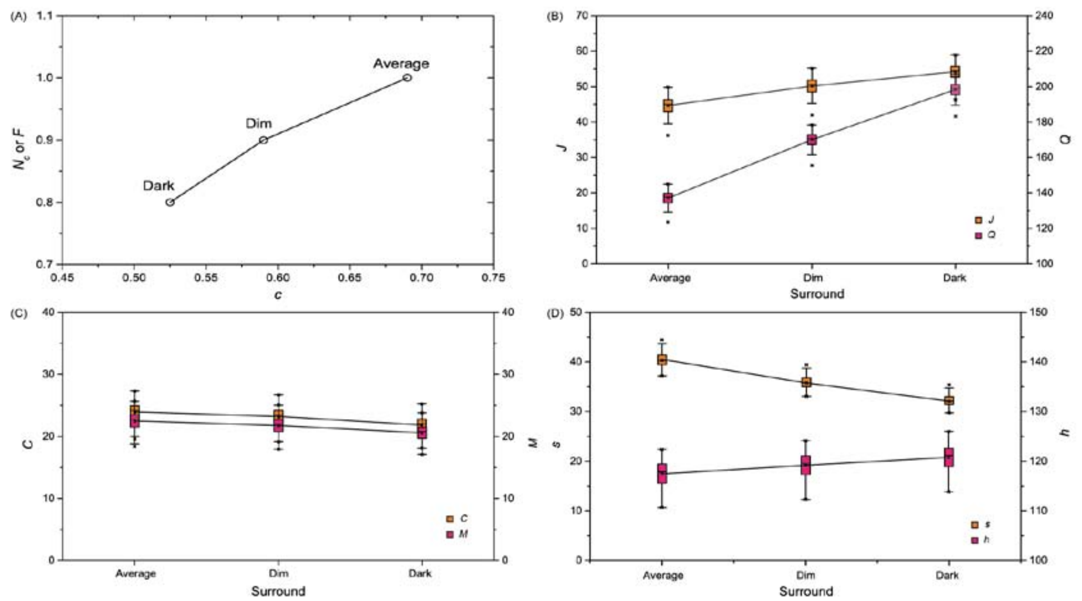

Figure 5: Effect of viewing surroundings on the color appearance of peridot. (A) Linear interpolation to obtain N_c and *F*. Relationship between viewing surrounds and lightness *J*, brightness *Q*; (B) chroma *C*, colorfulness *M*; (C) saturation *s*, and hue *h*; (D) of peridot are given.

simulate three luminance levels of environmental conditions.

The predictions indicate that lightness *J* and brightness *Q* of peridot rises significantly when the viewing surroundings become darker (Figure 5B). Chroma C and colorfulness M decrease slightly (Figure 5C), and saturation s falls (Figure 5D) which should be explained by the rapid rising of brightness. Hue h of peridot rises slightly when the viewing surroundings become darker (Figure 5D).

Taking an overall view of the predictions, a significant difference appears in lightness and brightness when the viewing surroundings change, which indicates that viewing surroundings mainly influence the lightness and brightness of peridot.

Conclusion

Chemical analysis and UV-vis spectra analysis showed there are seven narrow absorption bands at 414nm, 443nm, 481nm, 512nm, 557nm, 664nm and 684nm in peridot that should be assigned to the Fe chromophore. The color appearance of peridot will be brighter and more vivid when the luminance increases, which corresponds to Hunt Effect and Stevens Effect. Viewing surroundings have a great influence on the lightness and brightness in color appearance of peridot. CAM16 color appearance model is not suitable to predict the contributions of the light source on the color appearance of peridot due to the metameric effect. The windowing issue and the facets in peridot should be taken into consideration during the prediction calculation.

Acknowledgment

The experiments in this research were conducted in the Lab of Gemological Research at the School of Gemmology, China University of Geosciences, Beijing, China.

References

1. Koivula JI. San Carlos peridot. G&G. 1981; 17: 205-214.
2. Koivula JI, Fryer CW. The gemological charac-teristics of Chinese peridot. G&G. 1986; 22: 38-40.
3. Keller PC, Wang F. A survey of the gemstone resources of China. G&G. 1986; 22: 3-13.
4. Koivula JI, Kammerling RC, Fritsch E. More on peridot from Pakistan. G&G. 1994; 30: 275.
5. Koivula JI, Kammerling RC, Fritsch E.: Peridot from Pakistan. G&G. 1994; 30: 196.
6. Frazier S, Frazier A. The perils of peridot pursuit. The Lapidary Journal. 1997; 50: 18-23.
7. Bouilhol P, Burg JP, Bodinier JL, Schmidt MW, Bernasconi SM, Dawood H. Gem olivine and calcite mineralization precipitated from subduction-derived fluids in the Kohis-tan arc-mantle (Pakistan). The Canadian Mineralogist. 2012; 50: 1291-1304.
8. Scalisi P, Cook D. Classic Mineral Localities of the World. Van Nostrand Reinhold Co., New York. 1983.
9. Keller PC. Gemstones and Their Origins. Van Nostrand Reinhold Co., New York. 1990.
10. Kammerling RC, Scarratt K, Bosshart G, Jobbins AE, Kane RE, Gübelin EJ, et al. Myanmar and its gems-An update. Journal of Gemmology. 1994; 24: 3-40.
11. Kammerling RC, Koivula JI. A preliminary investigation of peridot from Vietnam. Journal of Gemmology. 1995; 24: 355-361.
12. Thuyet NTM, Hauzenberger C, Khoi NN, Diep CT, Lam CV, Minh NT, et al. Peridot from the central highlands of Vietnam: properties, origin, and formation. G&G. 2016; 52: 276-287.
13. Stockton CM, Manson DV. Peridot from Tanzania. G&G. 1983; 19: 103-107.
14. Keller PC. Gemstones of East Africa. Geoscience Press, Phoenix, AZ. 1992.
15. Gübelin EJ. Zabargad: The ancient peridot island in the Red Sea. G&G. 1981; 17: 2-8.
16. Adamo I, Bocchio R, Pavese A, Prosperi L. Characterization of peridot from Sardinia, Italy. G&G. 2009; 45: 130-133.
17. Gunawardene. Peridot from Ratnapura District, Sri Lanka. Journal of Gemmology. 1985; 19: 692-702.
18. Tang J, Guo Y, Xu C. Light Pollution Effects of Illuminance on Yellowish Green Forsterite Color under CIE Standard Light Source D65. EKOLOJI. 2018; 27: 1181-1190.
19. Tang J, Guo Y, Xu C. Color effect of light sources on peridot based on CIE1976 L*a*b* color system and round RGB diagram system. Col Res & Appl. 2019; 44: 932-940.
20. Tang J, Guo Y, Xu C. Metameric Effects on Peridot by Changing Background Color. JOSA. 2019; 36: 2030-2039.
21. Luo MR, Hunt RWG. The structures of the CIE 1997 color appearance model (CIECAM97s). Col Res & Appl. 1998; 23: 138-146.
22. Moroney N, Fairchild MD, Hunt RWG, Li CJ, Luo MR, Newman T. The CIECAM02 color appearance model. IS&T and SID 10th Color Imaging Conference. 2002. 23-27.
23. Commission Internationale de l'Eclairage, A Colour Appearance Model for Colour Management Systems: CIECAM02. Vienna: CIE. 2004.
24. Li CJ, Li Z, Wang Z, Xu Y, Luo MR, Cui G, et al. Comprehensive color solutions: CAM16, CAT16, and CAM16-UCS. Col Res & Appl. 2017; 42: 703-718.
25. Bai XQ, Liao NF. Research on Color Space Uniformity Based on New Color Appearance Model CAM16. Acta Optica Sinica. 2020; 40: 0433001.
26. Shi CJ, Zhu F. Research on Color Vision Differences of Observers Based on Color Appearance Model CIECAM02 and CIECAM16. Laser & Optoelectronics Progress. 2021; 58: 1933001.
27. Burns RG. Crystal field spectra and evidence of cation ordering in olivine minerals. AM. 1970; 55: 1608-1632.
28. Fairchild MD. Color appearance model. John Wiley & Sons. 2013.